Arch. Pharm. Chem. Life Sci. 2015, *348*, 730–742

ARCH PHARM
Archiv der Pharmazie

Full Paper

Synthesis of Tolmetin Hydrazide–Hydrazones and Discovery of a Potent Apoptosis Inducer in Colon Cancer Cells

Ş. Güniz Küçükgüzel[1], Derya Koç[1], Pelin Çıkla-Süzgün[1], Derya Özsavcı[2], Özlem Bingöl-Özakpınar[2], Pınar Mega-Tiber[3], Oya Orun[3], Pınar Erzincan[4], Safiye Sağ-Erdem[4], and Fikrettin Şahin[5]

[1] Department of Pharmaceutical Chemistry, Faculty of Pharmacy, Marmara University, Haydarpaşa, İstanbul, Turkey
[2] Department of Biochemistry, Faculty of Pharmacy, Marmara University, Haydarpaşa, İstanbul, Turkey
[3] Department of Biophysics, School of Medicine, Marmara University, Başıbüyük, İstanbul, Turkey
[4] Department of Chemistry, Faculty of Arts and Sciences, Marmara University, Göztepe, Istanbul, Turkey
[5] Department of Genetics and Bioengineering, Faculty of Engineering and Architecture, Yeditepe University, Kayışdağı, İstanbul, Turkey

Tolmetin hydrazide and a novel series of tolmetin hydrazide–hydrazones **4a–l** were synthesized in this study. The structures of the new compounds were determined by spectral (FT-IR, ^{1}H NMR) methods. *N*′-[(2,6-Dichlorophenyl)methylidene]-2-[1-methyl-5-(4-methylbenzoyl)-1*H*-pyrrol-2-yl]acetohydrazide (**4g**) was evaluated *in vitro* using the MTT colorimetric method against the colon cancer cell lines HCT-116 (ATCC, CCL-247) and HT-29 (ATCC, HTB-38) to determine growth inhibition and cell viability at different doses. Compound **4g** exhibited anti-cancer activity with an IC_{50} value of 76 μM against colon cancer line HT-29 (ATCC, HTB-38) and did not display cytotoxicity toward control NIH3T3 mouse embryonic fibroblast cells compared to tolmetin. In addition, this compound was evaluated for caspase-3, caspase-8, caspase-9, and annexin-V activation in the apoptotic pathway, which plays a key role in the treatment of cancer. We demonstrated that the anti-cancer activity of this compound was due to the activation of caspase-8 and caspase-9 involved in the apoptotic pathway. In addition, in this study, we investigated the catalytical effect of COX on the HT-29 cancer line, the apoptotic mechanism, and the moleculer binding of tolmetin and compound **4g** on the COX enzyme active site.

Keywords: Apoptosis / Caspase-3 / Colon cancer / Hydrazide–hydrazone / Tolmetin

Received: May 26, 2015; Revised: July 7, 2015; Accepted: July 21, 2015

DOI 10.1002/ardp.201500178

Additional supporting information may be found in the online version of this article at the publisher's web-site.

Introduction

Colorectal cancer is considered as the fourth leading cause of cancer deaths. The worldwide incidence of colorectal cancer is almost one million new malignant cases each year with a survival rate under 50%, despite the chemotherapy [1]. The high prevalence and mortality of colorectal cancer make the search for effective prevention and/or treatments an urgent medical concern. The use of chemopreventive approaches to control colon cancer is an attractive strategy. The relationship between inflammation and cancer is well established that

Correspondence: Prof. Ş. Güniz Küçükgüzel, Department of Pharmaceutical Chemistry, Faculty of Pharmacy, Marmara University, Haydarpaşa 34668, İstanbul, Turkey.
E-mail: gkucukguzel@marmara.edu.tr
Fax: +90-216-3452952

This work was partly presented at the 4th International Meeting on Pharmacy and Pharmaceutical Sciences, Istanbul, Turkey, 18–23 September 2014.

suggests the use of anti-inflammatory drugs for the prevention of colorectal cancer.

Non-steroidal anti-inflammatory drugs (NSAIDs) are a well-known class of anti-inflammatory drugs that inhibit the cyclooxygenase (COX) enzymes which are crucial for the production of eicosanoids from arachidonic acid [2]. Reports have shown the ability of many anti-inflammatory agents, especially the NSAIDs, to inhibit tumor growth. Moreover, several studies have revealed a substantial decrease in the mortality from colorectal cancer in association with the use of aspirin and other NSAIDs [3–5]. The mechanism of action that is responsible for the chemopreventive activity of NSAIDs is widely attributed to COX-2 inhibition [6–8] and a COX-2-independent mechanism [9–11]. In addition, tumor growth inhibition and apoptotic effect of the some compounds derived from NSAIDs has been reported [12–16] (Fig. 1).

Tolmetin, 2-[1-methyl-5-(4-methylbenzoyl)-1*H*-pyrrol-2-yl]-acetic acid, is a non-steroidal anti-inflammatory drug which inhibits prostaglandin synthesis and it has been reported to prevent proliferation of colon cancer cells. In addition, tolmetin's regulatory effects on anti-cancer drug therapy were studied. It was reported that tolmetin and other NSAIDs have effects on increasing the cytotoxic activity of the anti-cancer drugs [17]; they inhibit the β-catenin functions and that is why tolmetin can be used for developing new anti-cancer agents [18].

Hydrazide–hydrazones, which are intermediates in the synthesis of biologically active compounds, are widely drawing attention in the scientific community due to their several biological and clinical applications [12, 14, 19–21]. Activity of hydrazones is known to be associated with the active pharmacophoric group (–CONH–N=C<). In the light of these knowledge, 12 compounds which possess hydrazide–hydrazone as main structure have been synthesized in this study starting from tolmetin. 2-[1-Methyl-5-(4-methylbenzoyl)-1*H*-pyrrol-2-yl]-*N*′-[(pyridinyl/substitutedphenyl/2-furyl)methylidene]acetohydrazides (**4a–l**) were synthesized. Tolmetin (**1**) and tolmetin hydrazide–hydrazone **4g** were tested for their growth inhibitory and apoptotic activities against colorectal tumor cells.

Results and discussion

Chemistry

Twelve novel hydrazide–hydrazones have been synthesized from tolmetin hydrazide, which is a derivative of 2-[1-methyl-5-(4-methylbenzoyl)-1*H*-pyrrol-2-yl]acetic acid (tolmetin); an inhibitor of prostaglandine synthesis and a non-steroidal anti-inflammatory drug. Structures of the synthesized compounds were confirmed by UV, IR, ^{1}H NMR and LC-MS (EI) (only **3**) and their purity was checked by elemental analysis, TLC, and HPLC-diode array.

As shown in the synthesis scheme, tolmetin was first synthesized from tolmetin sodium dihydrate by hydrolyzing

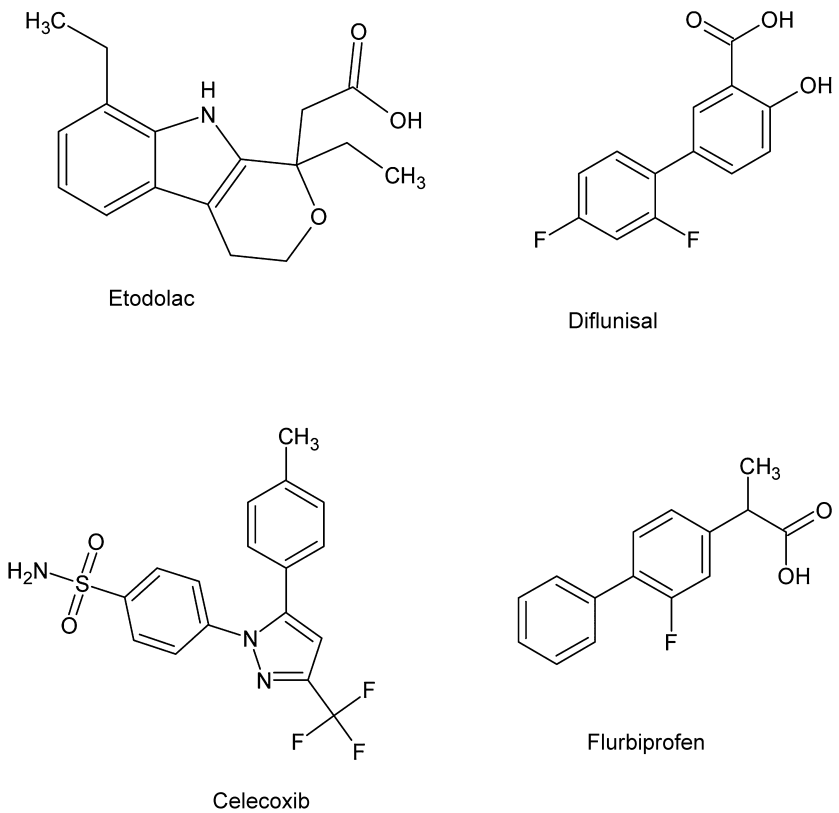

Figure 1. Tumor growth inhibiting NSAIDs (etodolac, celecoxib, diflunisal, flurbiprofen).

the dihydrate in acidic conditions. Methyl 2-[1-methyl-5-(4-methylbenzoyl)-1*H*-pyrrol-2-yl]acetate (**2**) has been synthesized from tolmetin (**1**) with methanol and few drops of concentrated sulfuric acid. 2-[1-Methyl-5-(4-methylbenzoyl)-1*H*-pyrrol-2-yl]acetohydrazide (**3**) was synthesized from compound **2**, which is an ester, with hydrazine hydrate and methanol. Compound **3**, tolmetin hydrazide derivative, was refluxed with substitued aldehydes and led us to the synthesis of 2-[1-methyl-5-(4-methylbenzoyl)-1*H*-pyrrol-2-yl]-*N*′-[(pyridinyl/substitutedphenyl/2-furyl)methylidene]acetohydrazides (**4a-l**), hydrazide–hydrazone compounds (Fig. 2).

Tolmetin sodium dihydrate was dissolved in water and 37% HCl was added until it stopped precipitating. The white precipitate was controlled with pH paper. Tolmetin yield was 95%. FT-IR spectrum data of 2-[1-methyl-5-(4-methylbenzoyl)-1*H*-pyrrol-2-yl]acetic acid (**1**) were observed 1688 cm^{-1}(C=O), 3370 cm^{-1} (O–H), and 1225 cm^{-1} (C–O) from carboxylic acid functional group [22]. 2-[1-Methyl-5-(4-methylbenzoyl)-1*H*-pyrrol-2-yl]acetic acid (tolmetin) was reacted with methanol in the presence of concentrated sulfuric acid, which leads to the synthesis of methyl 2-[1-methyl-5-(4-methylbenzoyl)-1*H*-pyrrol-2-yl]acetate (**2**). Compound **2** is not an original compound [23]. FT-IR spectrum of compound **3** showed 1720 cm^{-1} (C=O), 1205 cm^{-1} (C–O), both belong to ester functional group. Besides, 3370 cm^{-1} (O–H, carboxylic acid) disappeared. ^{1}H NMR spectrum of tolmetin ester was determined at 3.81 ppm (3H, s, $COOCH_3$) and there was no peak in the spectrum which belongs to OH proton of caboxylic acid group; which lead us to conclude that ester form of tolmetin was succesfully synthesized. Compound **3** is an original compound which was synthesized from methyl 2-[1-methyl-5-(4-methylbenzoyl)-1*H*-pyrrol-2-yl]acetate (**2**) in the presence of hydrazine–hydrate and methanol under reflux for 3 h and the yield was 84%. The UV spectrum of tolmetin hydrazide (**3**) established two maximum absorbance values at 254 and 300 nm in ethanol. The FT-IR spectrum of compound **3**

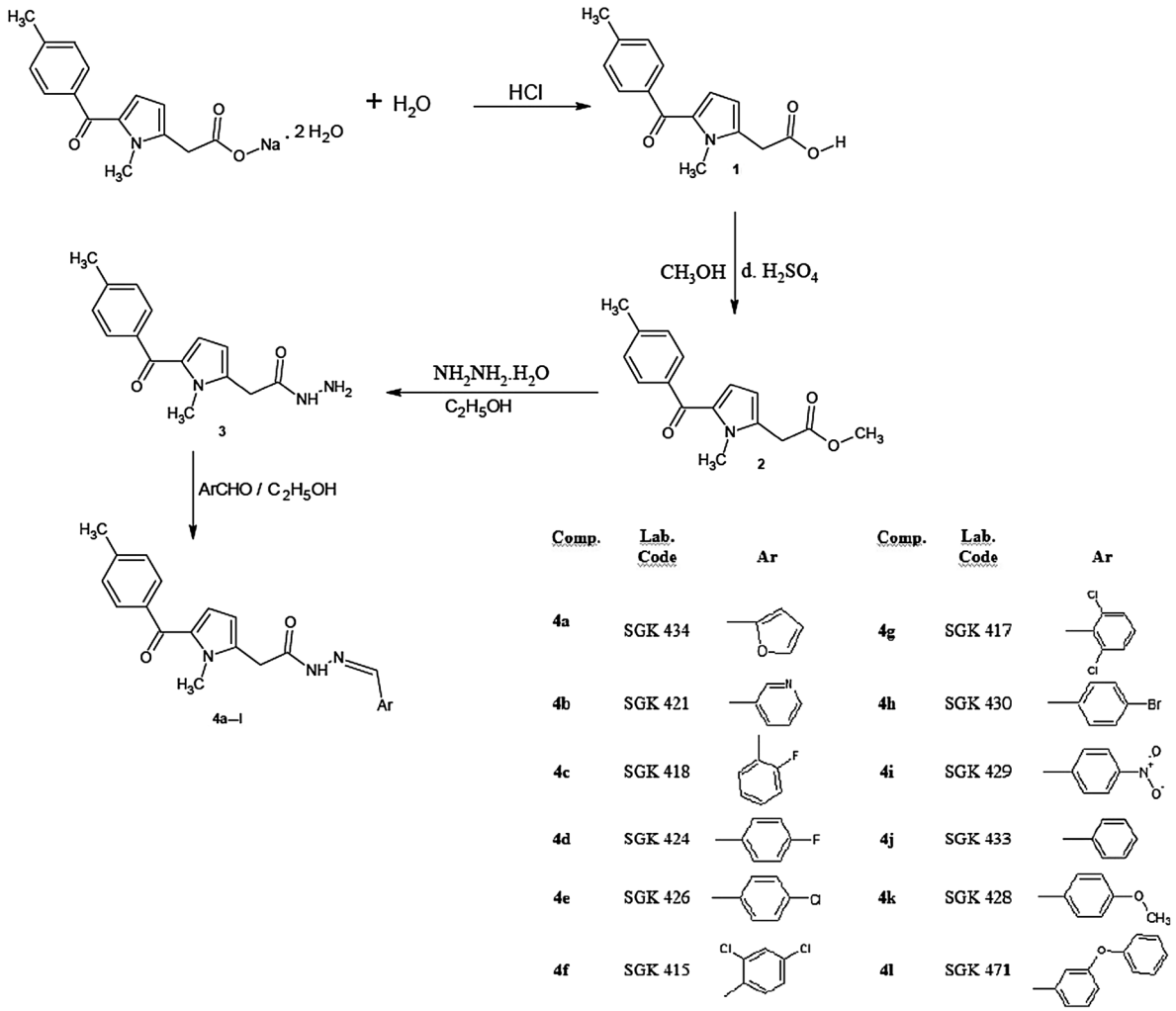

Comp.	Lab. Code	Ar	Comp.	Lab. Code	Ar
4a	SGK 434		4g	SGK 417	
4b	SGK 421		4h	SGK 430	
4c	SGK 418		4i	SGK 429	
4d	SGK 424		4j	SGK 433	
4e	SGK 426		4k	SGK 428	
4f	SGK 415		4l	SGK 471	

Figure 2. Synthetic route of tolmetin hydrazide–hydrazones (**4a–l**).

showed 3300 cm^{-1} ($CONHNH_2$), which proves the hydrogen bond in the compound and 1643 cm^{-1} (C=O, hydrazide) in compound **3**. ^1H NMR spectrum of compound **3** in DMSO-d_6 showed that methyl protons disappeared at 3.81 ppm (3H, s, $COOCH_3$). ^1H NMR spectrum of tolmetin hydrazide was observed at 4.27 ppm (1H, s, NH_2) and at 9.23 ppm (1H, s, NH). This information showed us that ester derivative was transformed to hydrazide derivative and $–CONHNH_2$ group was formed. Mass spectra of tolmetin hydrazide (**3**) with electron impact method were determined at *m/z* 271.1 as molecular ion peak and *m/z* 212.1 as base peak (100%).

2-[1-Methyl-5-(4-methylbenzoyl)-1*H*-pyrrol-2-yl]acetohydrazide (**3**) and substituted aldehydes were refluxed in the presence of ethanol for 2 h which led to the synthesis of hydrazide–hydrazone compounds **4a–l**, yield 50–93%. The FT-IR spectra of (**4a–l**) compounds showed 3069–3231 cm^{-1} (hydrazone, N–H). The C=O stretch band in hydrazone CONHN=CH structure (amide I band) and C=N stretch band were observed at 1660–1692 and 1597–1628 cm^{-1}, respectively. The low cm^{-1} N–H stretch bands were observed in some compounds, which lead us to the conclusion that some of the N–H groups had hydrogen bonds. ^1H NMR spectra of the compounds **4b–l** at 300 MHz frequency in $CDCl_3$, N–H protons, and azomethine (CH=N) protons were detected at 9.58–11.43 ppm (1H, s) and 7.79–8.20 ppm (1H, s), respectively. Besides that, pyrrole $N–CH_3$ (3H, s) and CH_2 protons were detected at 3.84–4.05 ppm and at 4.08–4.23 ppm (2H, s). The ^1H NMR spectra of tolmetin 2-furyl derivative (**4a**) were studied in DMSO-d_6 and hydrazone N–H proton was seen at 11.42–11.67 ppm (1H, s); CH=N proton was seen at 8.07–8.21 ppm (1H, s), respectively. In the light of foregoing and according to the literature [14, 24, 25], we assume that our compound chose the *E* isomer form as N–H protons were detected at 11.42 and 11.67 ppm. The two singlet peaks were observed because of the *cis/trans* conformers of the resonance form of the *E* isomer compound's amide. ^1H NMR spectra of the same compound showed that hydrazone N–H proton and CH=N proton were observed at 8.84 ppm (1H, s) and 7.65 ppm (1H, s), respectively. 2-Furfuryl derivative (**4a**) was studied by ^1H NMR at 600 MHz in DMSO-d_6 and the pyrole $N–CH_3$ peak was overlapped in the solution peak. As a result, its spectra were studied again in $CHCl_3$ and $N–CH_3$ peak was observed in 4.04 ppm.

Biological activity

In the present day, it is reported that tolmetin inhibits the growth of colon cancer cells [26]. On the light of foregoing, we aimed to investigate the anti-cancer activity of tolmetin hydrazide–hydrazone **4g**, which is an original compound and a derivative of tolmetin, a substance with reported anti-cancer activities human colon cancer cell lines, HCT-116 (ATCC, CCL-247) and HT-29 (ATCC, HTB-38) were used to investigate the anti-cancer effects of the compound. These studies were carried out at Department of Biochemistry, Faculty of Pharmacy, Marmara University. The evaluation of anti-cancer and cytotoxicity effects was performed by measuring the levels of alive cells after incubation with the tolmetin and compound **4g** using MTT colorimetric assay [27] against panel of human colon cancer cell lines. Tolmetin hydrazone (**4g**) was found to be active on HT-29 cell line with 76 μM of IC_{50} value. Furthermore, tolmetin hydrazide–hydrazone was found to be more active on HT-29 cancer cell line in higher doses as shown in Table 1 and Fig. 3.

It was acknowledged that cancer cells resist to the normal death pathways. Cancer cells use different mechanisms including extrinsic and intrinsic pathways to escape apoptosis. The evidence obtained in recent years indicates that many non-steroidal anti-inflammatory drugs (NSAIDs) have anti-proliferative activity in tumor cells [28, 29]. In the current study, we also investigated whether the anti-cancer effects of compound **4g** and tolmetin occurred via the apoptotic pathway and, if so, which signaling pathway that initiates apoptosis was activated in host defence.

Early stages of apoptosis are characterized by phosphatidylserine (PS) externalization on the outer surface of the plasma membrane [30]. To determine the effects of tolmetin and compound **4g** depending on doses on PS exposure, we used annexin V staining. According to our results, tolmetin and **4g** (SGK-417) increased PS externalization as compared with the control group but this increase was significantly greater for **4g** than tolmetin in 100 μM ($p < 0.001$) (Fig. 4).

After the flip floating of PS, apoptotic death signaling triggers and activates caspases. Caspases are known as

Table 1. Percentage of concentration-growth inhibition against HT-29 cell line.

Concentration	Growth inhibition (%)	
	Tolmetin	4g (SGK 417)
10^{-6}	17.58	21.3
10^{-5}	29.23	34.57
10^{-4}	34.15	50.66
10^{-3}	37.76	62.99
10^{-2}	41.62	70.23

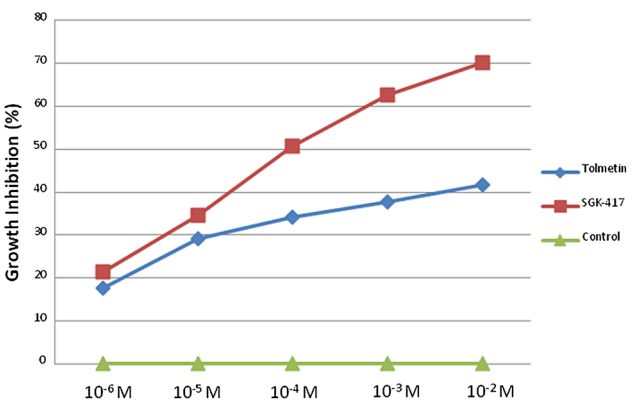

Figure 3. Cytotoxic activity of tolmetin and compound **4g** (SGK-417) on HT-29 cells.

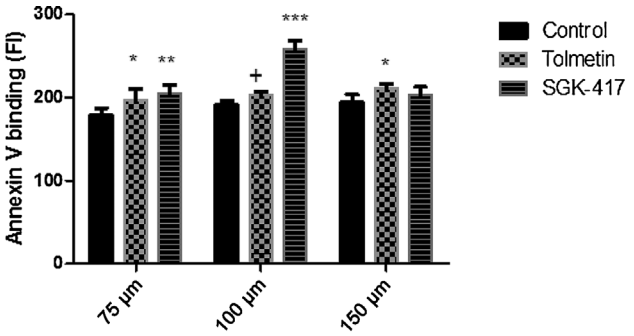

Figure 4. The early apoptotic effects of tolmetin and compound **4g** (SGK-417) on HT-29 cells. Data shown as mean ± SD in triplicate culture and a representative of two independent experiments. $^{*}p < 0.05$; $^{**}p < 0.001$; $^{***}p < 0.0001$ versus control; $^{+}p < 0.0001$ versus SGK-417.

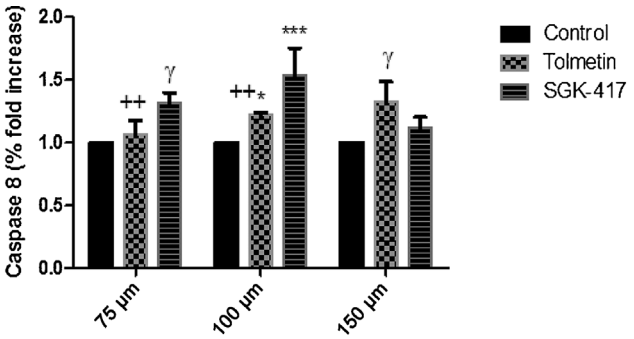

Figure 6. The effects of tolmetin and compound **4g** (SGK-417) on caspase 8 activity in HT-29 cells. Data shown as mean ± SD in triplicate culture and a representative of two independent experiments. $^{*}p < 0.05$; $^{***}p < 0.0001$; $^{\gamma}p < 0.01$ versus control; $^{++}p < 0.05$ versus SGK-417.

cysteine-proteases and play an important role in apoptosis. They normally exist in a precursor form that has little activity but once activated, breakdown structural elements and other proteins. Caspases 8 and 9 are known as initiator and caspase 3 is an effector protein in the apoptotic signaling pathways. Caspase 9 is predominantly defined in the intrinsic pathway and caspase 8 is described in the extrinsic pathway. Depending on the cell type and stimulus, the cells determine which caspases are used. Both pathways generally overlap downstream with the activation of caspases 3, 6, and 7 [31, 32].

Caspases 3, 8, and 9 enzyme levels were significantly increased in the colon cancer cells which were incubated with tolmetin (**1** (100 µM) and **4g** (SGK-417)) (Figs. 5–7). Loss of mitochondrial membrane potential is a hallmark of intrinsic apoptotic pathway. In this study, we also observed the effects of tolmetin and compound **4g** on the mitochondrial membrane potential as shown in Fig. 8, JC-1 fluorochrome staining. Moreover, we showed that both compounds

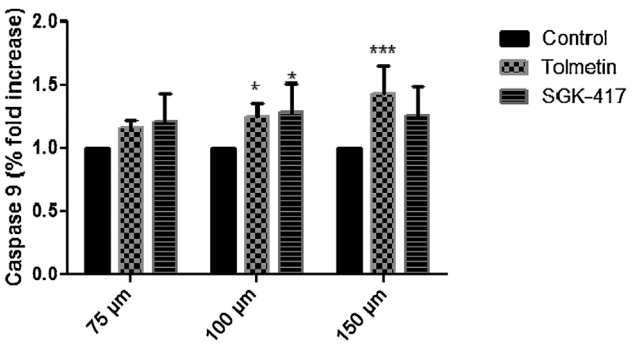

Figure 7. The effects of tolmetin and compound **4g** (SGK-417) on caspase 9 activity in HT-29 cells. Data shown as mean ± SD in triplicate culture and a representative of two independent experiments. $^{*}p < 0.05$; $^{***}p < 0.0001$ versus control.

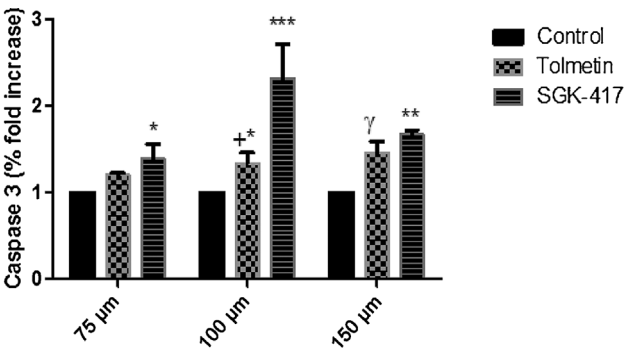

Figure 5. The effects of tolmetin and compound **4g** (SGK-417) on caspase 3 activity in HT-29 cells. Data shown as mean ± SD in triplicate culture and a representative of two independent experiments. $^{*}p < 0.05$; $^{**}p < 0.001$; $^{***}p < 0.0001$; $^{\gamma}p < 0.01$ versus control; $^{+}p < 0.0001$ versus **4g**.

induced disturbance of the mitochondrial membrane potential and activation of caspases 3, 8, and 9, all of which are involved in extrinsic and intrinsic apoptotic pathways.

COX-2 is induced in many inflammatory reactions. Recent studies report that COX-2 expression is abnormally elevated in some colon adenomas [33]. Various animal and human tumor tissues, including human colon cancer, contain high concentrations of prostaglandins. Therefore, these observations led us to investigate catalytical effects of COX enzymes on HT-29 cancer line.

Inhibitory action of tolmetin and **4g** was first observed using COX-1 standard provided by the kit. COX-1 inhibitor SC-560 and tolmetin inhibited COX-1 activity as expected. Total COX activity was very low in HT-29 cells (just above the basal level) for approximately 8×10^5 cells, where activity of MCF-7 cells were 1.3-fold higher with a half cell population (4×10^5 cells). There was no detectable change in the COX-activities after inhibitors were added, but the number of HT-29 cells was considerably reduced (Table 2). These results

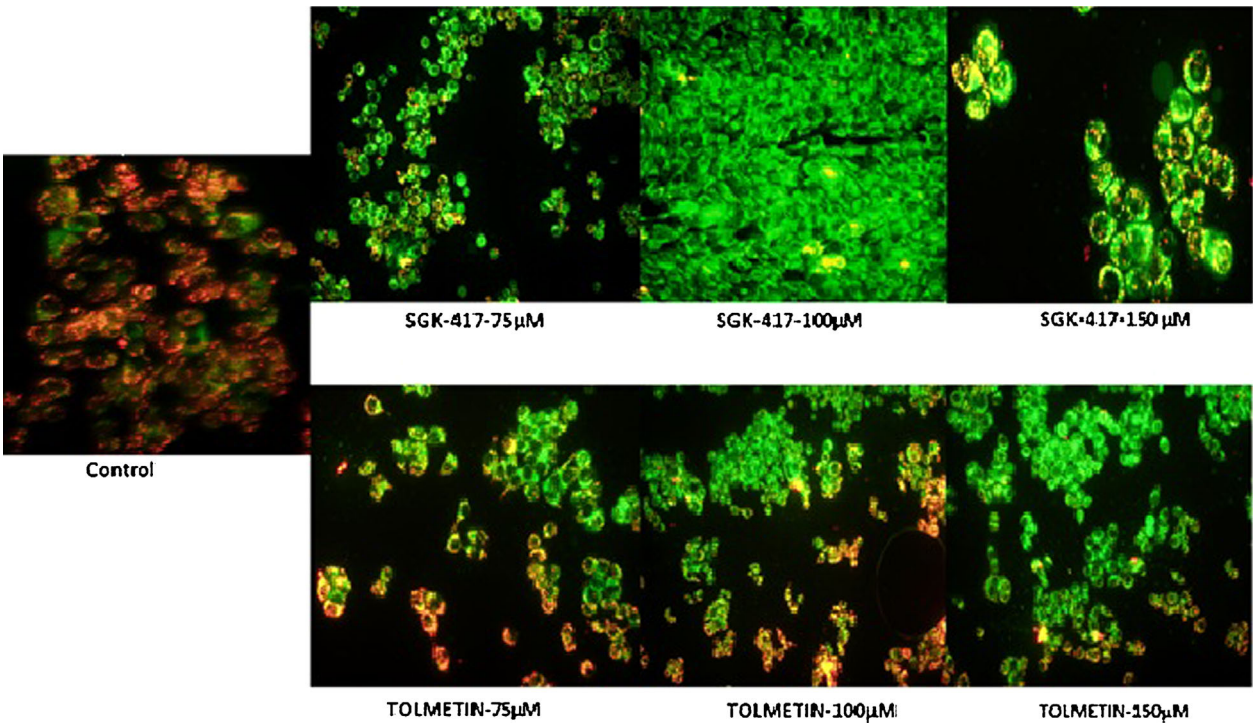

Figure 8. Fluorescence microscopy after JC-1 staining showing changes in the mitochondrial membrane potential in HT-29 cells; magnification: ×100).

encouraged us to investigate molecular binding of tolmetin and **4g** with COX enzyme active site.

In silico studies

COX-1 and COX-2 binding affinities of tolmetin and **4g** were explored with molecular docking using AutoDock Vina software [34] in order to get insight into the inhibitory binding mechanism. COX enzymes have two different catalytic sites: Cyclooxygenase active site is a hydrophobic channel elongated toward the membrane domain. It is the target of NSAID drugs. Peroxidase active site is situated at the surface of catalytic domain and contains a heme cofactor. Although the nature of substrate binding to cyclooxygenase site is well established, peroxidase site is less explored.

Table 2. COX activities and effect of inhibitors were determined both in isolated ovine COX-1 standard and two cancer cell lines, HT-29 and MCF-7.

	Total activity nmol/min/mL	% Decrease in Cox-activity	% Decrease in cell number with respect to control
COX-1 standard			
COX-1 Standard	23.20	–	
Std + DuP-697 (COX2 inh)	13.67	9.53	
Std + SC-560 (COX1 inh)	5.02	18.18	
Tolmetin	3.56	19.64	
4g	19.70	3.50	
Cancer cell lines			
HT-29-control	6.04	–	–
HT-29 + Tolmetin	6.17	0.00	55
HT-29 + **4g**	6.42	−0.25	60
MCF7-control	8.45	–	–
MCF7 + Tolmetin	8.33	0.25	41.1
MCF7 + **4g**	8.90	−0.32	0

However, it is known that both sites are involved in catalytic reaction [35].

According to AutoDock Vina docking scores, both tolmetin and **4g** are binded to COX-1 cyclooxygenase active site as well as to peroxidase active site. Binding energies for tolmetin and **4g** at COX-1 cyclooxygenase active site were calculated as −8.1 and −8.6 kcal/mol, respectively. Although **4g** exhibited slightly more binding affinity than tolmetin (elucidated by its smaller free energy of binding), these compounds showed less binding affinity to the cyclooxygenase active site of COX-1 enzyme relative to the reference pdb inhibitor α-methyl-4-biphenylacetic acid (the defluorinated analog of flurbiprofen) whose binding energy was calculated as −9.1 kcal/mol. These results are consistent with biological activity measurement. Binding mode of reference pdb inhibitor showed favorable π-alkyl interactions between its phenyl moiety and Leu352 and Leu531 residues in addition to H-bonding to Arg120. Binding orientations of tolmetin and **4g** in COX-1 are depicted in Fig. 9.

Figure 9 reveals that cyclooxygenase binding mechanisms of both compounds are dominated by hydrophobic interactions except one non-bonded attraction between $-CH_3$ hydrogen of pyrrole ring in tolmetin and –OH oxygen of Tyr355. Other favorable interactions responsible for binding of tolmetin are π-alkyl interactions between aromatic rings of tolmetin and alkyl groups of Leu531 and Leu352 residues similar to the reference inhibitor. Additionally, aromatic π-electrons of Trp387 and Tyr385 interact favorably with *para* CH_3 substituent in tolmetin. Similar to tolmetin, **4g** also fits cyclooxygenase active site mainly with hydrophobic interactions with Leu384, Leu352, and Ala527. Dichlorophenyl group of **4g** is surrounded by Ile523, Tyr355, Leu93, Ile89, and Val116 and exhibits π-cation interactions with Arg120 which is critical for slightly more favorable binding of **4g** with respect to tolmetin where dichlorophenyl moeity is absent.

As stated before, some conformers of tolmetin and **4g** also bind to peroxidase active site of COX-1. In the literature, there are several docking studies for various inhibitors binding to cyclooxygenase active site of COX enzymes [36]. However, as far as we know, peroxidase active site is less explored and inhibitors binding to peroxidase active site are not yet reported. According to AutoDock Vina scores, tometin and **4g** bound more favorably to peroxidase site than cyclooxygenase site of COX-1. The binding affinity of **4g** was even stronger than tolmetin as observed from the calculated binding energies of −9.7 and −8.8 kcal/mol, respectively.

Binding orientation of tolmetin and **4g** in peroxidase active site of COX-1 are illustrated in Fig. 10. Both tolmetin and **4g** exhibit favorable π–π stacking interactions with

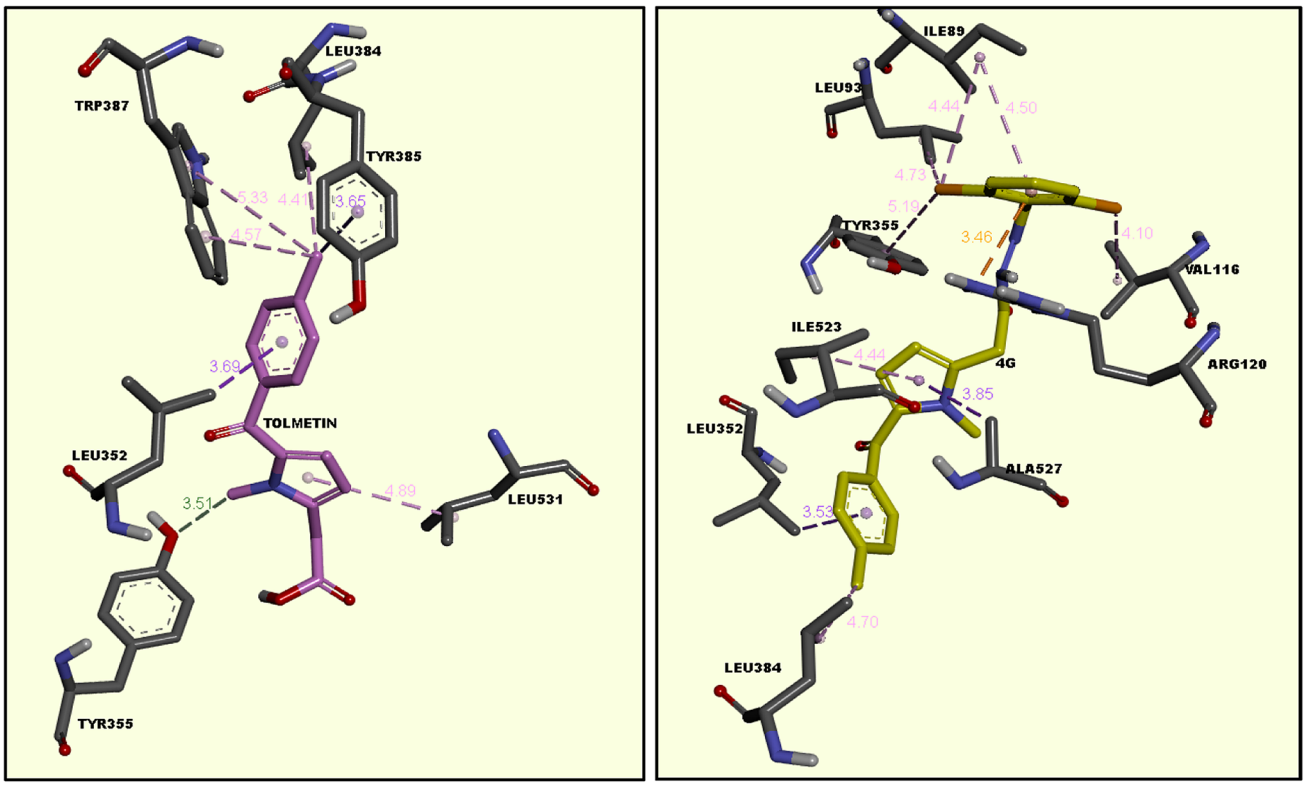

Figure 9. Binding orientation of tolmetin (left: pink) and **4g** (right: yellow) in the cyclooxygenase active site of COX-1. Interaction distances are given in Å.

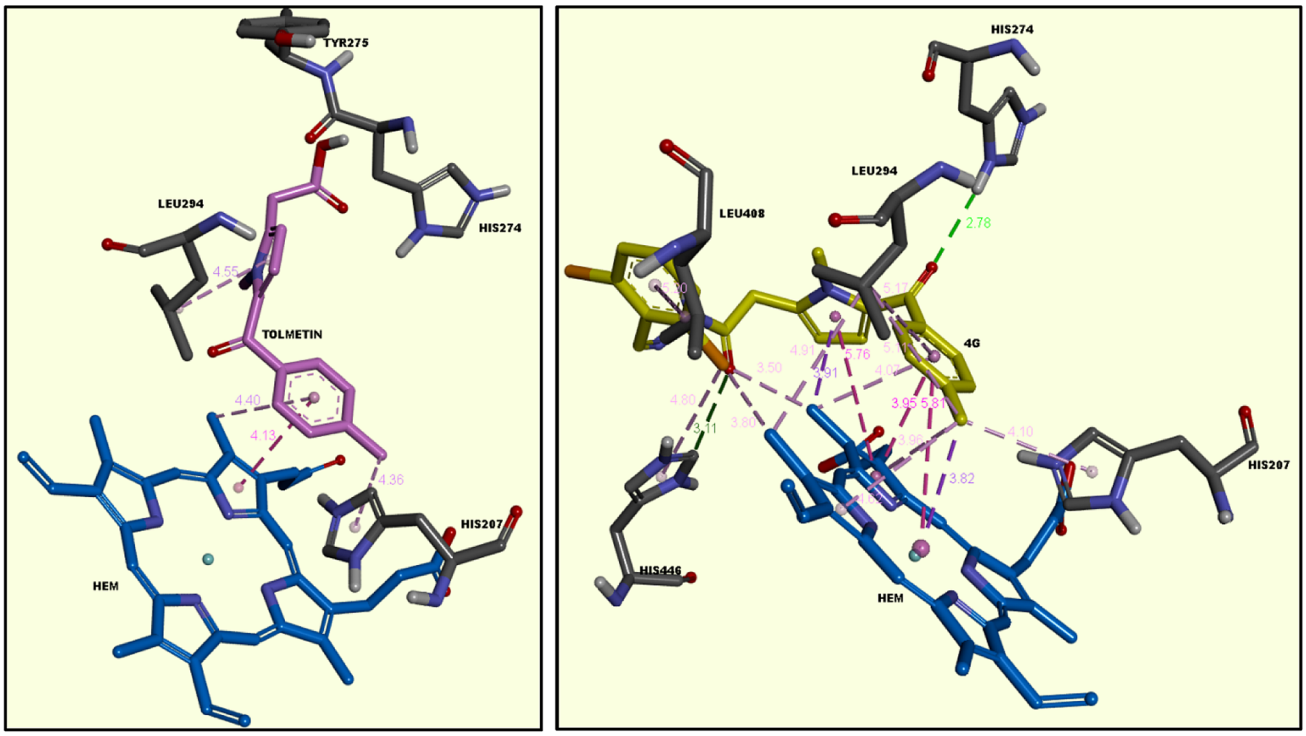

Figure 10. Binding orientation of tolmetin (left: pink) and **4g** (right: yellow) in the peroxidase active site of COX-1. Interaction distances are given in Å.

porphyrin ring of heme cofactor and π–alkyl interactions with His207 which is essential for peroxidase activity of COX-1. Additional interactions of **4g** responsible for its higher affinity are the strong H-bond with His274 (2.78 Å), and the interactions of chlorophenyl moiety with Leu408 and His446.

Tolmetin is known to be a selective COX1 inhibitor. In accordance with this, only a few conformers of tolmetin bound to COX-2 with the binding energy of −6.6 kcal/mol revealing a negligibly weak affinity. On the other hand, none of the conformers of **4g** exhibited binding to COX-2 indicating its higher selectivity to COX-1 with respect to tolmetin.

Conclusion

One of the beneficial methods of synthesizing a pro-drug is to hydrolyze the hydrazones and reveal its active metabolite, therefore, we can block the $-NH_2$ group and have compounds that are less toxic than hydrazides [37]. In the recent studies, researchers focus on synthesizing more active, less toxic chemotherapeutics and this led them to the synthesis of new hydrazide–hydrazones compounds. Both the anti-cancer activity and the apoptotic effects of these molecules are popular studies [38].

HCT-116 (ATCC, CCL-247) and HT-29 (ATCC, HTB-38) human colon cancer cell lines are used for the studies of tolmetin (**1**) which was also reported to be active in colon cancer and compound **4g** for their anti-cancer activity at Department of Biochemistry, Marmara University. Therefore, whether hydrazone functionality increases the anti-cancer activity or not comparing to tolmetin was studied. According to MTT assays, compound **4g** was found to be more active than tolmetin only in HT-29 cancer cell line, in a dose-dependent manner with IC_{50} value of 76 μM.

Caspase-3 is an enzyme catalyzing specific cell key protein division and is mostly induced fatal protease. This activation starts with caspase-8 and caspase-9 shred. Caspase-8 is a basic compound for exogenous cell death pathway by TNF family members. Caspase-9 is a key compound for mitochondrial (endogenous) pathway. Caspase-9 activates the other caspases. To evaluate the apoptotic mechanisms which are important in cancer formation, caspase activities were studied in HT-29 cell line (according to MTT assay) and the changes in the levels of caspase 3, 8, and 9 were observed. For this study, 75, 100, and 150 μM concentrations of compounds **1** and **4g** were used. Annexin V, which is a protein existing on the surface of the cells that undergo apoptosis, was also used to determine early apoptosis in the cells [39].

In the light of foregoing, compound **4g**, bearing hydrazone functionality, triggers apoptosis by affecting caspase 3 levels and does that by using caspase 8 and caspase 9 pathways in cancer cells. It is also observed that HT-29 colon cancer cells which are treated with **4g** and undergo

ARCH PHARM
Archiv der Pharmazie

apoptosis, have high levels of annexin V with the dose of 75–100 μM.

We believe that anti-colon cancer activity will exist in tolmetin chromophore group as a result of the HT-29 anti-cancerogenic activity of both tolmetin and tolmetin hydrazone **4g**, which activates caspases 3, 8, and 9; effective enzymes in apoptosis pathway.

Docking calculations predicted compound **4g** as a selective inhibitor of COX-1. Despite its smaller affinity to cyclooxygenase site of the enzyme, it binds to peroxidase site more favorably. Owing to this ability, it is expected to have a different mode of action than other NSAIDs drugs. It can be a potent novel therapeutic agent—by inducing apoptosis in HT-29 cells through activation of caspases and that this activation involves COX-1-mediated mechanisms.

Experimental

Chemistry

All chemicals were purchased from Merck, Sigma–Aldrich, or Fluka. Reactions were monitored by TLC on silica gel plates purchased from Merck. Melting points of the synthesized compounds were determined in a Schmelzpunktbestimmer SMPII melting point apparatus and are uncorrected. The purity of the compounds was checked on TLC plates pre-coated with silica gel G using the solvent systems M_1 (chloroform/methanol 40:60 v/v), M_2 (petroleum ether/ethyl acetate 50:50 v/v), and M_3 (petroleum ether/ethyl acetate 30:70 v/v). The spots were located under UV light (254 nm) ($T = 21°C$). The liquid chromatographic system consists of an Agilent Technologies 1100 series instrument equipped with a quaternary solvent delivery system and a model Agilent series G1315 A photodiode array detector. A Rheodyne syringe loading sample injector with a 50-μL sample loop was used for the injection of the analytes. Chromatographic data were collected and processed using Agilent Chemstation Plus software. The separation was performed at ambient temperature using a normal phase Ace 3 C18 (10 cm × 4.0 mm). All experiments were performed in gradient mode. The mobile phase was prepared by mixing acetonitrile/distilled water (50:50) (v/v) for all compounds filtered through a 0.45-μm pore filter and subsequently degassed by ultrasonication, prior to use. Solvent delivery was employed at a flow rate of 1 mL/min. Detection of the analytes was carried out at 254 nm. Elemental analyses were performed on a CHNS-932 (LECO). FT-IR spectra were recorded on a Shimadzu FT-IR-8400S spectrophotometer. ^{1}H NMR spectra were recorded on Bruker 300 MHz Ultrashield TM and Bruker 600 MHz UltrashieldPlus TM (300 MHz) NMR spectrometers using $CDCl_3$ as solvent. MALDI-TOF HR-MS spectra using the EI ionization techniques were performed using a Jeol JMS-700 instrument. Chemical shifts (δ) are reported in parts per million (ppm). Data are reported as follows: chemical shift, multiplicity (s: singlet, d: doublet, m: multiplet, and t: triplet), coupling constants (Hz), and integration.

*2-[1-Methyl-5-(4-methylbenzoyl)-1H-pyrrol-2-yl]acetic acid (**1**)*

Tolmetin sodium dihydrate (0.01 mol) was dissolved in distilled water (22 mL). HCl (37%) was added on the resulting solution until completion of the deposition process, and was controlled with litmus paper blue. The resulting white precipitate was filtered, washed with distilled water, dried, and crystallized from ethanol. MW: 257.284. m.p. 157°C. Yield 95%. Rf × 100 value 70 (M_1). HPLC t_R (min): 1.006. IR (ν_{max}, cm^{-1}): 3370 (carboxylic acid OH), 1688 (C=O).

*Methyl 2-[1-methyl-5-(4-methylbenzoyl)-1H-pyrrol-2-yl]-acetate (**2**)*

Tolmetin (0.01 mol) and methanol (20 mL) were refluxed for 3 h in a few drops of concentrated sulfuric acid. The contents of the flask were subsequently cooled and neutralized by using $NaHCO_3$ (5%). The resulting precipitate was filtered, dried, and recrystallized twice from ethanol. Cream-colored solid. MW: 271.311. m.p. 121–123°C [35]. Yield 77%. Rf × 100 value 32 (M_2). HPLC t_R (min): 3.369. UV (EtOH) λ_{max} nm: 318, 311, 299, 256. IR (ν_{max}, cm^{-1}): 1720 (ester C=O), 1205 (ester C–O). ^{1}H NMR (300 MHz, DMSO-d_6): δ (ppm) 2.49 (3H, s, Ar-C$\underline{H}_3$); 3.66 (3H, s, N–C$\underline{H}_3$); 3.81 (3H, s, O–C$\underline{H}_3$); 3.90 (2H, s, –C$\underline{H}_2$–); 6.11 (1H, d, pyrrole ring protons adjacent CH_2, $J = 3.9$ Hz); 6.56 (1H, d, pyrrole ring protons adjacent C=O, $J = 3.9$ Hz); 7.29 (2H, d, benzene ring o-protons by methyl, $J = 7.81$ Hz); 7.29 (2H, d, benzene ring o-protons by methyl, $J = 7.81$ Hz); 7.62 (2H, d, benzene ring o-protons by carbonyl, $J = 7.81$ Hz).

*2-[1-Methyl-5-(4-methylbenzoyl)-1H-pyrrol-2-yl]-acetohydrazide (**3**)*

To a methanolic solution of compound **2** (50 mL, 0.01 mol) was added hydrazine–hydrate (80%, 5 mL) and refluxed for 3 h. The reaction mixture was then cooled. The precipitated solid was washed with water, dried, and recrystallized twice from ethanol. Cream-colored solid. MW: 271.31438. m.p. 185–186°C. Yield 84%. Rf × 100 value 24.5 (M_3). HPLC t_R (min): 1.093. UV (EtOH) λ_{max} nm: 320, 312, 300, 254. FT-IR (ν_{max}, cm^{-1}): 3329, 3254 (hydrazide NH), 1643 (C=O). ^{1}H NMR (300 MHz, DMSO-d_6): δ (ppm) 2.37 (3H, s, Ar-C$\underline{H}_3$); 3.52 (2H, s, –C$\underline{H}_2$–CO–); 3.86 (3H, s, N–C$\underline{H}_3$); 4.27 (2H, s, –N$\underline{H}_2$); 6.06 (1H, d, pyrrole ring protons adjacent CH_2, $J = 3.9$ Hz); 6.54 (1H, d, pyrrole ring protons adjacent C=O, $J = 3.9$ Hz); 7.29 (2H, d, benzene ring o-protons by methyl, $J = 7.81$ Hz); 7.61 (2H, d, benzene ring o-protons by carbonyl, $J = 8.3$ Hz); 9.23 (1H, s, –N$\underline{H}$). MS [EI, m/z, (%)]: 271.1 [M^+] (% 62), 240.1 (% 18), 212.1 (% 100), 119 (% 27), 91 (% 14).

*General procedure for the synthesis of 2-[1-methyl-5-(4-methylbenzoyl)-1H-pyrrol-2-yl]-N′-[(pyridinyl/substituted phenyl/2-furyl)methylidene]acetohydrazides (**4a–l**)*

A solution of compound **3** (0.0025 mol) was dissolved in ethanol (20 mL) and equimolar amounts of appropriate aromatic aldehyde in absolute ethanol were heated under

reflux for 2 h. The obtained precipitate was filtered off, dried, and recrystallized twice from ethanol.

*N′-[Furan-2-yl-methylidene]-2-[1-methyl-5-(4-mehylbenzoyl)-1H-pyrrol-2-yl]acetohydrazide (**4a**)*
Cream-colored solid. MW: 349.38316. m.p. 222–224°C. Yield 93%. Rf × 100 value: 28 (M_2). HPLC t_R (min): 2.732. FT-IR (ν_{max}, cm^{-1}): 3183 (hydrazone NH), 1665 (C=O), 1620 (C=N). ^{1}H NMR (600 MHz, DMSO-d_6): δ (ppm) 2.36 (3H, s, Ar-C$\underline{H}_3$); 3.84 (in solvent peak N–C$\underline{H}_3$); 4.07 (2H, s, –C$\underline{H}_2$–); 6.10–7.58 (9H, m, protons of pyrrole and furan ring, Ar–H); 8.07, 8.21 (1H, ss, –C$\underline{H}$=N); 11.42,11.67 (1H, ss, –N$\underline{H}$). Anal. calcd. for $C_{20}H_{19}N_3O_3$: C, 68.75; H, 5.48; N, 12.03%. Found: C, 68.24; H, 5.25; N, 11.89%.

*2-[1-Methyl-5-(4-methylbenzoyl)-1H-pyrrol-2-yl]-N′-[pyridin-3-yl-methylidene]acetohydrazide (**4b**)*
Cream-colored solid. MW: 392.451. m.p. 191–193°C. Yield 74%. Rf × 100 value: 17 (M_2). HPLC t_R (min): 2.007. FT-IR (ν_{max}, cm^{-1}): 3069 (hydrazone NH), 1676 (C=O), 1604 (C=N). ^{1}H NMR (300 MHz, $CDCl_3$): δ (ppm) 1.78 (s, –C$\underline{H}_3$ peak of ethanol held by the molecule); 2.44 (3H, s, Ar–C$\underline{H}_3$); 3.83 (s, –C$\underline{H}_2$ peak of ethanol that held by the molecule); 3.97 (s, –O$\underline{H}$ peak of ethanol that held by the molecule); 4.04 (3H, s, N–C$\underline{H}_3$); 4.22 (2H, s, –C$\underline{H}_2$–); 6.19 (1H, d, pyrrole ring protons adjacent CH_2, J = 4.06 Hz); 6.71 (1H, d, pyrrole ring protons adjacent C=O, J = 4.04 Hz); 7.24–7.74; 8.02–8.06 (8H, m, Ar–H); 7.89 (1H, s, –C$\underline{H}$=N); 10.16 (1H, s, –N$\underline{H}$). Anal. calcd. for $C_{21}H_{20}N_4O_2.1/2H_2O.1/2C_2H_5OH$: C, 67.33; H, 6.16; N, 14.28%. Found: C, 67.73; H, 5.52; N, 15.17%.

*N′-[(2-Fluorophenyl)methylidene]-2-[1-methyl-5-(4-methylbenzoyl)-1H-pyrrol-2-yl]acetohydrazide (**4c**)*
Cream-colored solid. MW: 400.445. m.p. 185°C. Yield 50%. Rf × 100 value: 32 (M_2). HPLC t_R (min): 3.760. FT-IR (ν_{max}, cm^{-1}): 3192 (hydrazone NH), 1674 (C=O), 1628 (C=N). ^{1}H NMR (300 MHz, $CDCl_3$): δ (ppm) 1.66 (s, –C$\underline{H}_3$ peak of ethanol held by the molecule); 2.44 (3H, s, Ar–C$\underline{H}_3$); 3.83 (s, –C$\underline{H}_2$ peak of ethanol that held by the molecule); 3.99 (s, –O$\underline{H}$ peak of ethanol that held by the molecule); 4.05 (3H, s, N–C$\underline{H}_3$); 4.21 (2H, s, –C$\underline{H}_2$–); 6.19 (1H, d, pyrrole ring protons adjacent CH_2, J = 4.05 Hz); 6.71 (1H, d, pyrrole ring protons adjacent C=O, J = 4.05 Hz); 7.10–7.44 (8H, m, Ar–H); 8.09 (1H, s, –C$\underline{H}$=N); 9.58 (1H, s, –N$\underline{H}$). Anal. calcd. for $C_{22}H_{20}FN_3O_2.1/2C_2H_5OH$: C, 68.98; H, 5.79; N, 10.49%. Found: C, 69.33; H, 5.28; N, 11.03%.

*N′-[(4-Fluorophenyl)methylidene]-2-[1-methyl-5-(4-methylbenzoyl)-1H-pyrrol-2-yl]acetohydrazide (**4d**)*
Cream-colored solid. MW: 400.445. m.p. 200–201°C. Yield 83%. Rf × 100 value: 30 (M_2). HPLC t_R (min): 3.705. FT-IR (ν_{max}, cm^{-1}): 3227 (hydrazone NH), 1682 (C=O), 1603 (C=N). ^{1}H NMR (300 MHz, $CDCl_3$): δ (ppm) 1.7 (s, –C$\underline{H}_3$ peak of ethanol held by the molecule); 2.44 (3H, s, Ar–C$\underline{H}_3$); 3.81 (s, –C$\underline{H}_2$ peak of ethanol that held by the molecule); 3.97 (–O$\underline{H}$ peak of ethanol that held by the molecule); 4.04 (3H, s, N–C$\underline{H}_3$); 4.21 (2H, s, –C$\underline{H}_2$–); 6.19 (1H, d, pyrrole ring protons adjacent CH_2, J = 4.05 Hz); 6.72 (1H, d, pyrrole ring protons adjacent C=O, J = 4.05 Hz); 7.07–7.75 (8H, m, Ar–H); 7.84 (1H, s, –C$\underline{H}$=N); 10.10 (1H, s, –N$\underline{H}$). Anal. calcd. for $C_{22}H_{20}FN_3O_2.1/2C_2H_5OH$: C, 68.98; H, 5.79; N, 10.49%. Found: C, 69.04; H, 5.33; N, 11.33%.

*N′-[(4-Chlorophenyl)methylidene]-2-[1-methyl-5-(4-methylbenzoyl)-1H-pyrrol-2-yl]acetohydrazide (**4e**)*
Cream-colored solid. MW: 416.900. m.p. 198–200°C. Yield 70%. Rf × 100 value: 45 (M_2). HPLC t_R (min): 4.323. FT-IR (ν_{max}, cm^{-1}): 3154 (hydrazone NH), 1684, 1666 (C=O), 1597 (C=N). ^{1}H NMR (300 MHz, $CDCl_3$): δ (ppm) 1.67 (s, –C$\underline{H}_3$ peak of ethanol held by the molecule); 2.44 (3H, s, Ar–C$\underline{H}_3$); 3.82 (s, –C$\underline{H}_2$ peak of ethanol that held by the molecule); 3.98 (s, –O$\underline{H}$ peak of ethanol that held by the molecule); 4.04 (3H, s, N–C$\underline{H}_3$); 4.21 (2H, s, –C$\underline{H}_2$–); 6.18 (1H, d, pyrrole ring protons adjacent CH_2, J = 4.06 Hz); 6.71 (1H, d, pyrrole ring protons adjacent C=O, J = 4.04 Hz); 7.24–7.75 (8H, m, Ar–H); 7.82 (1H, s, –C$\underline{H}$=N); 9.97 (1H, s, –N$\underline{H}$). Anal. calcd. for $C_{22}H_{20}ClN_3O_2.1/2C_2H_5OH$: C, 66.26; H, 5.56; N, 10.08%. Found: C, 65.74; H, 5.070; N, 10.51%.

*N′-[(2,4-Dichlorophenyl)methylidene]-2-[1-methyl-5-(4-methylbenzoyl)-1H-pyrrol-2-yl]acetohydrazide (**4f**)*
Cream-colored solid. MW: 451.345. m.p. 202–206°C. Yield 82%. Rf × 100 value: 50 (M_2). HPLC t_R (min): 5.083. FT-IR (ν_{max}, cm^{-1}): 3140 (hydrazone NH), 1692 (C=O), 1597 (C=N). ^{1}H NMR (300 MHz, $CDCl_3$): δ (ppm) 1.66 (s, –C$\underline{H}_3$ peak of ethanol held by the molecule); 2.44 (3H, s, Ar–C$\underline{H}_3$); 3.82 (s, –C$\underline{H}_2$ peak of ethanol that held by the molecule); 3.98 (s, –O$\underline{H}$ peak of ethanol that held by the molecule); 4.03 (3H, s, N–C$\underline{H}_3$); 4.19 (2H, s, –C$\underline{H}_2$–); 6.16 (1H, d, pyrrole ring protons adjacent CH_2, J = 4.06 Hz); 6.70 (1H, d, pyrrole ring protons adjacent C=O, J = 4.05 Hz); 7.24–7.93 (7H, m, Ar–H); 8.20 (1H, s, –C$\underline{H}$=N); 9.81 (1H, s, –N$\underline{H}$). Anal. calcd. for $C_{22}H_{19}Cl_2N_3O_2.1/2C_2H_5OH$: C, 61.20; H, 4.91; N, 9.31%. Found: C, 60.75; H, 4.42; N, 9.65%.

*N′-[(2,6-Dichlorophenyl)methylidene]-2-[1-methyl-5-(4-methylbenzoyl)-1H-pyrrol-2-yl]acetohydrazide (**4g**)*
Cream-colored solid. MW: 428.311. m.p. 225–226°C. Yield 86%. Rf × 100 value: 60 (M_2). HPLC t_R (min): 4.683. UV (EtOH) λ_{max} nm: 310, 259, 220, 200. FT-IR (ν_{max}, cm^{-1}): 3184 (hydrazone NH), 1660 (C=O), 1622 (C=N). ^{1}H NMR (300 MHz, $CDCl_3$): δ (ppm) 2.44 (3H, s, Ar–C$\underline{H}_3$); 4.01 (3H, s, N–C$\underline{H}_3$); 4.20 (2H, s, –C$\underline{H}_2$–); 6.19 (1H, d, pyrrole ring protons adjacent CH_2, J = 4.06 Hz); 6.70 (1H, d, pyrrole ring protons adjacent C=O, J = 4.05 Hz); 7.24–7.74 (7H, m, Ar–H); 8.13 (1H, s, –C$\underline{H}$=N); 9.79 (1H, s, –N$\underline{H}$). Anal. calcd. for $C_{22}H_{19}C_{l2}N_3O_2$: C, 61.69; H, 4.47; N, 9.81%. Found: C, 60.84; H, 4.44; N, 9.83%.

*N′-[(4-Bromophenyl)methylidene]-2-[1-methyl-5-(4-methylbenzoyl)-1H-pyrrol-2-yl]acetohydrazide (**4h**)*
Cream-colored solid. MW: 461.351. m.p. 206–207°C. Yield 70%. Rf × 100 value: 35 (M_2). HPLC t_R (min): 4.489. FT-IR (ν_{max}, cm^{-1}): 3152 (hydrazone NH), 1686 (C=O), 1597 (C=N). ^{1}H NMR (300 MHz, $CDCl_3$): δ (ppm) 1.69 (s, –C$\underline{H}_3$ peak of ethanol held by the molecule); 2.44 (3H, s, Ar–C$\underline{H}_3$); 3.81 (s, –C$\underline{H}_2$ peak of

ARCH PHARM
Archiv der Pharmazie

ethanol that held by the molecule); 3.97 (s, –OH peak of ethanol that held by the molecule); 4.04 (3H, s, N–CH_3); 4.21 (2H, s, –CH_2–); 6.18 (1H, d, pyrrole ring protons adjacent CH_2, $J = 4.06$ Hz); 6.71 (1H, d, pyrrole ring protons adjacent C=O, $J = 4.05$ Hz); 7.24–7.74 (8H, m, Ar–H); 7.80 (1H, s, –CH=N); 10.08 (1H, s, –NH). Anal. calcd. for $C_{22}H_{20}BrN_3O_2.1/2C_2H_5OH$: C, 60.28; H, 4.60; N, 9.59%. Found: C, 59.54; H, 4.57; N, 9.62%.

*2-[1-Methyl-5-(4-methylbenzoyl)-1H-pyrrol-2-yl]-N′-[(4-nitrophenyl)methylidene]acetohydrazide (**4i**)*
Pale yellow colored solid. MW: 413.427. m.p. 225–228°C. Yield 88%. Rf × 100 value: 34 (M_2). HPLC t_R (min): 3.299. FT-IR (ν_{max}, cm^{-1}): 3180 (hydrazone NH), 1670 (C=O), 1599 (C=N). ^{1}H NMR (300 MHz, $CDCl_3$): δ (ppm) 2.32 (3H, s, Ar–CH_3); 3.90 (3H, s, N–CH_3); 4.08 (2H, s, –CH_2–); 6.04 (1H, d, pyrrole ring protons adjacent CH_2, $J = 4.06$ Hz); 6.58 (1H, d, pyrrole ring protons adjacent C=O, $J = 4.04$ Hz); 7.12–7.81; 8.11–8.23 (8H, m, Ar–H); 7.95 (1H, s, –CH=N); 11.43 (1H, s, –NH). Anal. calcd. for $C_{22}H_{20}N_4O_4.1/2H_2O$: C, 63.91; H, 5.12; N, 13.55%. Found: C, 64.49; H, 4.95; N, 13.73%.

*2-[1-Methyl-5-(4-methylbenzoyl)-1H-pyrrol-2-yl]-N′-[phenylmethylidene]acetohydrazide (**4j**)*
Cream-colored solid. MW: 382.45526. m.p. 168–172°C. Yield 71%. Rf × 100 value: 36 (M_2). HPLC t_R (min): 3.590. FT-IR (ν_{max}, cm^{-1}): 3194 (hydrazone NH), 1667 (C=O), 1605 (C=N). ^{1}H NMR (300 MHz, $CDCl_3$): δ (ppm) 1.68 (s, –CH_3 peak of ethanol held by the molecule); 2.44 (3H, s, Ar–CH_3); 3.83 (s, –CH_2 peak of ethanol that held by the molecule); 3.98 (s, –OH peak of ethanol that held by the molecule); 4.05 (3H, s, N–CH_3); 4.23 (2H, s, –CH_2–); 6.20 (1H, d, pyrrole ring protons adjacent CH_2, $J = 4.06$ Hz); 6.72 (1H, d, pyrrole ring protons adjacent C=O, $J = 4.04$ Hz); 7.24–7.75 (9H, m, Ar–H); 7.85 (1H, s, –CH=N); 9.82 (1H, s, –NH). Anal. calcd. for $C_{22}H_{21}N_3O_2.1/2C_2H_5OH$: C, 72.23; H, 6.32; N, 10.99%. Found: C, 72.32; H, 5.761; N, 11.65%.

*N′-[(4-Methoxyphenyl)methylidene]-2-[1-methyl-5-(4-methylbenzoyl)-1H-pyrrol-2-yl]acetohydrazide (**4k**)*
Cream-colored solid. MW: 412.481. m.p. 189°C. Yield 84%. Rf × 100 value: 31 (M_2). HPLC t_R (min): 3.460. FT-IR (ν_{max}, cm^{-1}): 3186 (hydrazone NH), 1668 (C=O), 1622 (C=N). ^{1}H NMR (300 MHz, $CDCl_3$): δ (ppm) 1.71 (s, –CH_3 peak of ethanol held by the molecule); 2.44 (3H, s, Ar–CH_3); 3.81 (s, –CH_2 peak of ethanol that held by the molecule); 3.84 (3H, s, N–CH_3); 3.98 (s, –OH peak of ethanol that held by the molecule); 4.05 (3H, s, –OCH_3); 4.21 (2H, s, –CH_2–); 6.20 (1H, d, pyrrole ring protons adjacent CH_2, $J = 4.06$ Hz); 6.71 (1H, d, pyrrole ring protons adjacent C=O, $J = 4.05$ Hz); 6.89–7.75 (8H, m, Ar–H); 7.80 (1H, s, –CH=N); 9.84 (1H, s, –NH). Anal. calcd. for $C_{23}H_{23}N_3O_3.1/2C_2H_5OH$: C, 69.88; H, 6.35; N, 10.19%. Found: C, 70.67; H, 5.876; N, 10.94%.

*2-[1-Methyl-5-(4-methylbenzoyl)-1H-pyrrol-2-yl]-N′-[3-phenoxyphenyl-methylidene]acetohydrazide (**4l**)*
White-colored solid. MW: 474.550. m.p. 172°C. Yield 62%. Rf × 100 value: 67 (M_2). HPLC t_R (min): 4.958. FT-IR (ν_{max}, cm^{-1}): 3231 (hydrazone NH), 1682 (C=O), 1612 (C=N). ^{1}H NMR (300 MHz, $CDCl_3$): δ (ppm) 1.66 (s, –CH_3 peak of ethanol held by the molecule); 2.44 (3H, s, Ar–CH_3); 3.81 (s, –CH_2 peak of ethanol that held by the molecule); 3.97 (s, –OH peak of ethanol that held by the molecule); 4.00 (3H, s, N–CH_3); 4.16 (2H, s, –CH_2–); 6.14 (1H, d, pyrrole ring protons adjacent CH_2, $J = 4.07$ Hz); 6.68 (1H, d, pyrrole ring protons adjacent C=O, $J = 4.06$ Hz); 7.07–7.74 (13H, m, Ar–H); 7.79 (1H, s, –CH=N); 9.77 (1H, s, –NH). Anal. calcd. for $C_{28}H_{25}N_3O_3.1/2C_2H_5OH$: C, 73.4; H, 5.95; N, 8.85%. Found: C, 73.76; H, 5.51; N, 9.26%.

Biological methods

Cell treatment

Human colon carcinoma cell lines HCT-116 (ATCC, CCL-247) and HT-29 (ATCC, HTB-38), and mouse embryonic fibroblast cell line NIH3T3 (ATCC, CRL-1658) were maintained in Dulbecco modified Eagle's medium (DMEM) supplemented with 10% FBS and 1% penicillin/streptomycin in the presence of 5% CO_2 in air at 37°C. Tolmetin and compound **4g** were dissolved in DMSO and the cells were treated with increasing doses of compounds for 24 h in 37°C. After the incubation, the cells were harvested to analyze apoptosis.

Cell viability assay

Cell viability was determined by the MTT assay method. Briefly, HT-29 cells (1×10^4 cells/well) were seeded into 96-well plates and incubated for 24 h at 37°C in CO_2 incubator. Then, the cells were grown in the absence or presence of increasing doses of tolmetin and compound **4g** at 37°C. After 24 h treatment, the media was removed and then 10 μL of MTT (5 mg/mL in phosphate-buffered saline) was added to each well for an additional 4 h. The precipitated formazan was dissolved in 100 μL of 10% SDS and the absorbance was taken at 570 nm. The percentage of viability was calculated as the following formula: (viable cells)% = (OD of treated sample/OD of untreated sample) × 100.

Annexin V binding

After treatment, the cells were pre-incubated on ice for 30 min. Then, cells were centrifuged and resuspended in cold PBS. Following incubation with annexin V for 30 min, the cells were subsequently washed and fixed in PFA. The fluorescence intensity was measured using a fluorospectrophotometer.

Measurement of caspase-3 activity

To quantify caspase-3 activity, a caspase colorimetric assay kit (Caspase-3 Cellular Activity Assay Kit, Millipore) was used. Firstly, tissue samples were sonicated in iced lysis buffer for 10 min. Caspase-3 activity was measured spectrophotometrically using tetrapeptide substrate *N*-acetyl-Asp-Glu-Val-Asp-*p*-nitroanilide (AC-DEVD-pNa) in the cytosolic samples. Briefly, the recommended amount of sample was added into each well and treated with assay buffer containing 400 μM substrate (DEVD-pNA) [100 mmol/L NaCl, 50 mmol/L HEPES, 10 mmol/L dithiothreitol, 1 mmol/L EDTA, 10% glycerol, 0.1% of 3-((3-cholamidopropyl)dimethylammonio)-1-propanesulfonic acid, pH 7.4]; then the microplate was equilibrated at

37°C for 10 min. The conversion of substrate into the colored product was measured and recorded at 30-min intervals for 2 h at 405 nm with a microplate reader [40].

Measurement of caspases 8 and 9 activity
To measure caspase 8 and caspase 9 activity, caspase colorimetric assay kits (Millipore, Billerica, MA) were used. Therefore, cell pellets were lysed in the lysis buffer, and supernatants were collected. The approximate amount of samples were incubated with reaction buffer and colorimetric substrate, acetyl (Ac)-Ile-Glu-Thr-Asp (IETD)-*p*-nitroaniline (pNA) for caspase-8 and Ac-Leu-Glu-His-Asp (LEHD)-pNA for caspase-9, respectively, at 37°C for 2 h in the dark. The reactions were assessed for changes in absorbance at 405 nm using a microplate reader. Results are expressed as fold increase of the activity measured in samples. Fold-increase activity can be determined by comparing the results of treated samples with the level of the uninduced control [41].

Determination of the mitochondrial membrane potential changes using fluorescent probe JC-1
JC-1, a lipophilic cationic dye, is widely used to detect mitochondrial depolarization. In healthy cells, the dye stains the mitochondrial membrane bright red whereas apoptotic cells were stained green. Briefly, cells were cultured on cover slips and exposed to drugs for 24 h. After discarding the culture medium, 1 mL of the JC-1 staining solution was added to the wells. The cells were then incubated at 37°C for 15 min in a CO_2 incubator and washed twice with assay buffer. A drop of assay buffer was then added to the wells prior to immediate examination in the fluorescence microscope (Olympus, Tokyo, Japan).

COX activity determination
COX activity of the samples was determined using COX activity assay kit (Cayman Chemicals) according to the kit's manual. Inhibitors were added in 100 μM concentration to the cultures and incubated for 24 h. Cells ($>5 \times 10^5$) were scraped and lysed with sonication. Reactivity was measured by detecting absorbance at 590 nm using a plate reader (Synergy H1, Biotek).

Docking procedure

AutoDock Vina software was employed for all protein-ligand docking calculations of flexible ligand in rigid protein [34]. The crystal structures of COX-1 [35] (PDB entry code: 1Q4G, resolution 2.0 Å, co-crystallized with the inhibitor α-methyl-4-biphenylacetic acid) and COX-2 [42] (PDB entry code: 3NT1, resolution 1.73 Å, co-crystallized with the inhibitor naproxen) were obtained from the Protein Data Bank. The PDB files were edited. The B-chains of each enzyme, water molecules, co-crystallized inhibitors α-methyl-4-biphenylacetic acid, and naproxen were deleted together with other compounds (detergents, glycerol used as a cryoprotectant during diffraction experiments) in the structure. The 3D structures of inhibitors in pdb files of COX enzymes, tolmetin, and **4g** were optimized with semiempirical PM6 method [43] via conformation search in Spartan 10 program [44]. For each compound, the most stable conformation was chosen and used for initial geometry in docking calculation. The AutoDock Tools program [45] was utilized to generate the docking input files as described before [46]. A grid box size of $40 \times 40 \times 40$ points in *x*, *y*, and *z* dimensions was built. For COX-1 target, the grid was centered at 26.108 (*x*), 35.061 (*y*), and 197.448 (*z*). Regarding COX-2, the grid was centered at −39.746 (*x*), −50.781 (*y*), and −22.645 (*z*). A grid spacing of 0.375 Å was used for the calculation of the energetic map. Ligands were chosen fully flexible. The Vina parameter "exhaustiveness" was set to the value of 10. The charge of the heme Fe atom was set to +2 manually. The resultant structure files were analyzed using Accelrys Discovery Studio Visualizer 4.1 program [47]. In order to validate the docking protocol, the co-crystallized inhibitors α-methyl-4-biphenylacetic acid and naproxen were docked into their respective enzymes COX-1 and COX-2. The docking poses were alligned to their binding orientation in the pdb files. Their docked poses were in perfect agreement with pdb poses, validating our procedure.

This work was generously supported by the Research Fund of Marmara University, project number: SAG-C-YLP-161111-0297. The authors are grateful to Dr. Jürgen Gross from the Institute of Organic Chemistry, University of Heidelberg, for his generous help on obtaining HR-EI/FAB mass spectra of the synthesized compounds. Tolmetin was supplied by Santa-Farma Pharmaceutical Industry Inc. S. S. Erdem thanks Prof. M. T. Saçan for the use of Spartan software.

The authors have declared no conflicts of interest. The authors alone are responsible for the content and writing of this article.

References

[1] D. Beck, P. Roberts, J. Rombeau, M. Stamos, S. Wexner, Colorectal cancer: epidemiology, etiology, and molecular basis, in *The ASCRS Manual of Colon and Rectal Surgery* (Eds.: S. D. Wexner, M. J. Stamos, J. Rombeau, P. L. Roberts, D. E. Beck), Springer, New York **2009**, pp. 463–484.
[2] J. R. Vane, R. M. Botting, *Scand. J. Rheumatol.* **1996**, *25*, 9–21.
[3] G. A. Kune, S. Kune, L. F. Watson, *Cancer. Res.* **1988**, *48*(15), 4399–4404.
[4] M. J. Thun, M. M. Namboodiri, C. W. Heath, *N. Engl. J. Med.* **1991**, *325*(23), 1593–1596.
[5] E. Giovannucci, E. B. Rimm, M. J. Stampfer, G. A. Colditz, A. Ascherio, W. C. Willett, *Ann. Intern. Med.* **1994**, *121*(4), 241–246.
[6] D. Wang, R. N. DuBois, *Oncogene* **2009**, *29*(6), 781–788.

[7] R. E. Harris, *Inflammopharmacology* **2009**, *17*(2), 55–67.
[8] Z. Khan, N. Khan, R. P. Tiwari, N. K. Sah, G. Prasad, P. S. Bisen, *Curr. Drug. Targets.* **2011**, *12*(7), 1082–1093.
[9] S. Grösch, T. J. Maier, S. Schiffmann, G. Geisslinger, *J. Natl. Cancer Inst.* **2006**, *98*(11), 736–747.
[10] R. Narayanan, H. N. Kim, N. K. Narayanan, D. Nargi, B. Narayanan, *Int. J. Oncol.* **2012**, *40*(1), 13–20.
[11] T. O. Ishikawa, H. R. Herschman, *Carcinogenesis* **2010**, *31*(4), 729–736.
[12] P. Çıkla, D. Özsavcı, Ö. Bingöl-Özakpınar, A. Sener, Ö. Cevik, S. Özbaş-Turan, J. Akbuğa, F. Sahin, Ş. G. Küçükgüzel, *Arch. Pharm.* **2013**, *346*(5), 367–379.
[13] Ş. G. Küçükgüzel, İ. Coşkun, S. Aydın, G. Aktay, Ş. Gürsoy, Ö. Çevik, Ö. Bingöl-Özakpınar, D. Özsavcı, A. Şener, N. Kaushik-Basu, A. Basu, T. T. Talele, *Molecules* **2013**, *18*(3), 3595–3614.
[14] S. Aydın, N. Kaushik-Basu, P. Arora, A. Basu, D. B. Nichols, T. T. Talele, M. Akkurt, İ. Çelik, O. Büyükgüngör, Ş. G. Küçükgüzel, *Marmara Pharm. J.* **2013**, *1*(17), 26–34.
[15] P. Çıkla, E. Tatar, İ. Küçükgüzel, F. Şahin, D. Yurdakul, A. Basu, R. Krishnan, D. B. Nichols, N. Kaushik-Basu, Ş. G. Küçükgüzel, *Med. Chem Res.* **2013**, *22*, 5685–5699.
[16] S. Aydın, N. Kaushik-Basu, S. Özbaş-Turan, J. Akbuğa, P. Mega Tiber, O. Orun, K. R. Gurukumar, A. Basu, Ş. G. Küçükgüzel, *Lett. Drug Des. Discov.* **2014**, *11*(2), 121–131.
[17] C. P. Duffy, C. J. Elliott, R. A. O'Connor, M. M. Heenan, S. Coyle, I. M. Cleary, K. Kavanagh, S. Verhaegen, C. M. O'Loughlin, R. NicAmhlaoibh, M. Clynes, *Eur. J. Cancer* **1998**, *34*(8), 1250–1259.
[18] D. Lu, H. B. Cottam, M. Corr, D. A. Carson, *Proc. Natl. Acad. Sci. USA* **2005**, *102*(51), 18567–18571.
[19] S. Rollas, Ş. G. Küçükgüzel, *Molecules* **2007**, *12*, 1910–1939.
[20] Ş. G. Küçükgüzel, E. E. Oruç, S. Rollas, F. Şahin, A. Özbek, *Eur. J. Med. Chem.* **2002**, *37*(3), 197–206.
[21] Ş. G. Küçükgüzel, A. Mazi, F. Sahin, S. Öztürk, J. Stables, *Eur. J. Med. Chem.* **2003**, *38*, 1005–1013.
[22] J. R. Carson, D. N. McKinstry, S. Wong, *J. Med. Chem.* **1971**, *14*(7), 646–647.
[23] H. Bundgaard, N. M. Nielsen, *Int. J. Pharm.* **1988**, *43*(1–2), 101–110.
[24] J. Easmon, G. Puerstinger, T. Roth, H. H. Fiebig, M. Jenny, W. Jaeger, G. Heinisch, J. Hofmann, *Int. J. Cancer* **2001**, *94*(1), 89–96.
[25] J. Easmon, G. Pürstinger, K. S. Thies, G. Heinisch, J. Hofmann, *J. Med. Chem.* **2006**, *49*(21), 6343–6350.
[26] L. J. Hixson, D. S. Alberts, M. Krutzsch, J. Einsphar, K. Brendel, P. H. Gross, N. S. Paranka, M. Baier, S. Emerson, R. Pamukcu, R. W. Burt, *Cancer Epidem. Biomar. Prev.* **1994**, *3*, 433–438.
[27] H. J. Woerdenbag, T. A. Moskal, N. Pras, T. M. Malingre, *J. Nat. Prod.* **1993**, *56*(6), 849–856.
[28] A. K. Claudius, C. S. Kankipati, R. S. Kilari, S. Hassan, K. Guest, S. T. Russell, C. J. Perry, L. A. Stark, I. D. Nicholl, *Oncol. Rep.* **2014**, *32*(4), 1670–1680.
[29] V. V. Sahasrabuddhe, M. Z. Gunja, B. I. Graubard, B. Trabert, L. M. Schwartz, Y. Park, A. R. Hollenbeck, N. D. Freedman, K. A. McGlynn, *J. Natl. Cancer. Inst.* **2012**, *104*(23), 1808–1814.
[30] M. D. Jacobson, J. F. Burne, M. C. Raff, *EMBO J.* **1994**, *13*, 1899–910.
[31] S. Nagata, *Cell* **1997**, *88*, 355–365.
[32] S. Kumar, *Cell Death Differ.* **2007**, *14*, 32–43.
[33] H. Sano, K. Kawahito, R. L. Wilder, A. Hashiramoto, S. Mukai, K. Asai, S. Kimura, H. Kato, M. Kondo, T. Hla, *Cancer Res.* **1995**, *55*, 3785–3789.
[34] O. Trott, A. J. Olson, *J. Comput. Chem.* **2010**, *31*, 455–461.
[35] K. Gupta, B. S. Selinsky, C. J. Kaub, A. K. Katz, P. J. Loll, *J. Mol. Biol.* **2004**, *335*, 503–518.
[36] a) G. H. Hegazy, H. I. Ali, *Bioorg. Med. Chem.* **2012**, *20*, 1259–1270. b) P. Yadav, P. Singh, A. K. Tewari, *Bioorg. Med. Chem.Lett.* **2014**, *24*, 2251–2255. c) G. S. Hassan, S. M. Abou-Seria, G. Kamel, M. M. Ali, *Eur. J. Med. Chem.* **2014**, *76*, 482–493. d) K. Ozadalı, F. Ozkanlı, S. Jain, P. P. N. Rao, C. A. Velazquez-Martinez, *Bioorg. Med. Chem.* **2012**, *20*, 202912–2922. e) O. Ünsal-Tan, K. Ozadalı, K. Piskin, A. Balkan, *Eur. J. Med. Chem.* **2012**, *57*, 59–64. f) O. Ünsal-Tan, K. Özden, A. Rauk, A. Balkan, *Eur. J. Med. Chem.* **2010**, *45*, 2345–2352.
[37] S. Rollas, Ş. G. Küçükgüzel, *Open. Drug. Deliv. J.* **2008**, *2*, 77–85.
[38] J. Hofmann, G. Heinisch, J. Easmon, G. Pürstinger, H. H. Fiebig, US 7,112,680. **2006**.
[39] Y. Zhao, J. Hui, D. Wang, L. Zhu, J. H. Fang, X. D. Zhao, *Chem. Pharm. Bull.* **2010**, *58*, 1324–1327.
[40] B. Gao, H. L. Shi, X. Li, S. P. Qiu, H. Wu, B. B. Zhang, X. J. Wu, Z. T. Wang, *Life Sci.* **2014**, *108*, 63–70.
[41] Z. Li, Q. Gao, *Anim. Cells. Syst.* **2013**, *17*, 147–153.
[42] K. C. Duggan, M. J. Walters, J. Musee, J. M. Harp, J. R. Kiefer, J. A. Oates, L. J. Marnett, *J. Biol. Chem.* **2010**, *285*, 34950–34959.
[43] J. J. P. Stewart, *J. Mol. Model.* **2007**, *13*(12), 1173–1213.
[44] Wavefunction Inc., 2014. Spartan 14, Irvine, CA, USA. Available from: http://www.wavefun.com
[45] G. M. Morris, R. Huey, W. Lindstrom, M. F. Sanner, R. K. Belew, D. S. Goodsell, A. J. Olson, *J. Comp. Chem.* **2009**, *16*, 2785–2791.
[46] S. S. Erdem, S. Türkkan, K. Yelekçi, N.-G. Kelekçi, *J. Neural Transm.* **2013**, *120*, 859–862.
[47] Accelrys Software Inc., 2013. Discovery Studio Modeling Environment, Release 4.0, San Diego.